



國立臺灣大學
National Taiwan University

Dealing with the large scale structure inhomogeneity

Fabien Nugier

法比恩

LeCosPA

National Taiwan University

Center for High Energy Physics, HEP Group Seminar
12th September, 2017 – Chung Yuan Christian University, Taiwan

The large scale structure

(Very) tentative definition :

“Everything above galaxy scale that is sensitive to gravitational instability.”

2dFGRS (2002) :

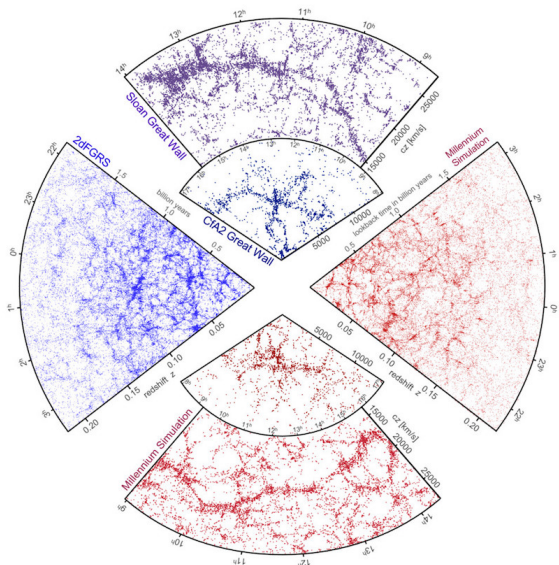
- 2.5 Gly depth on 2 slices
- ~ 1500 sqdeg area
- spectra for $\sim 250k$ objects
- <http://www.2dfgrs.net/>

Millennium Run (2005) :

- 10 G particles
- 2 Mly box
- ~ 20 M galaxies

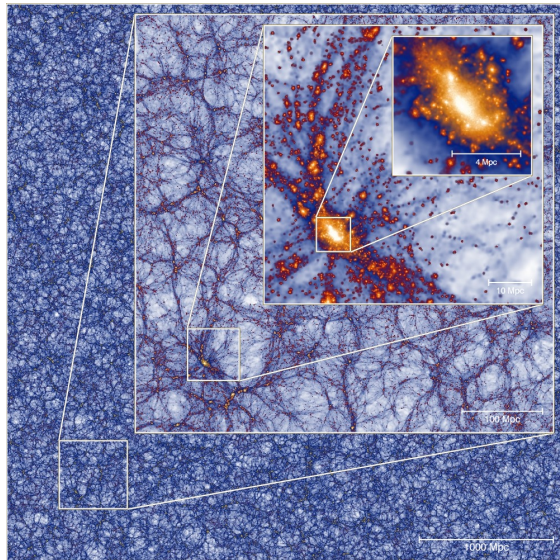
Sloan Digital Sky Survey :

- 3 M spectra
- $\sim 35\%$ of the sky



Millennium-XXL (2010)

- 300 billion particles
whole Univ. to $z \sim 0.72$
- goal 1 : relation between optical richness, lensing mass, X-ray luminosity and thermal Sunyaev-Zeldovich (tSZ) signal from CMB
- goal 2 : mass of extreme galaxy clusters
- **useful of other probes :**
BAOs, redshift space distortions (RSD), cluster number counts, weak gravitational lensing (WL), integrated Sachs-Wolfe (ISW) effect.
- halo mass function, power spectrum
- gives optical, lensing, X-ray, tSZ maps, galaxy clusters catalogues

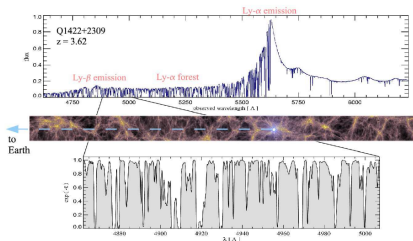


See [Angulo et al. 2013](#).

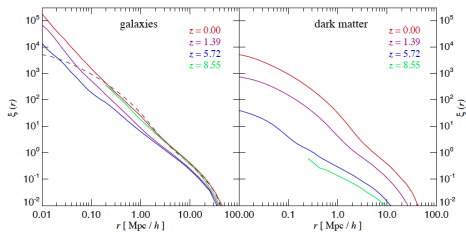
Examples of other probes

Source of images : [Springel, Frenk, White 2006](#)

- Intergalactic H absorption lines in quasar spectra \Rightarrow Lyman- α forest.



- 2pt-correlation (of galaxies or dark matter) \Leftrightarrow Power spectrum / BAO.



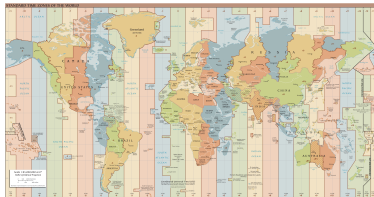
◀ ◻ ▶ ◀ ◻ ▶ ◀ ≡ ▶ ◀ ≡ ▶ ≡ ≡ ≡ ↺ 🔍 ↻

Two aspects of this talk

- **RELATIVISTIC CORRECTIONS DUE TO THE LSS :**
how does the LSS affects cosmological observables, how we can use adapted coordinates which actually simplify calculations.
- **COMPARING SUPERNOVAE DATA AND LSS IN OUR LOCAL UNIVERSE :**
what can we learn by comparing these probes, what it can say about the H_0 tension, supernovae or galaxy catalogues.

Adapted coordinates as a tool

IDEA : Simplify relativistic calculations by working in coordinates defined from observable (and thus gauge-invariant) quantities.



- 1938 : Temple's ‘optical co-ordinates’
- 1958 : Joseph’s “optical co-ordinates”
- 1968 : Saunders “observer’s polar coordinates”
- 1984 : Maartens detailed “observational coordinates”
- 2011 : “Geodesic light-cone coordinates”
- Numerical implementations of Bester, Larena, Bishop ’13 & ’15

Geodesic Light Cone coordinates

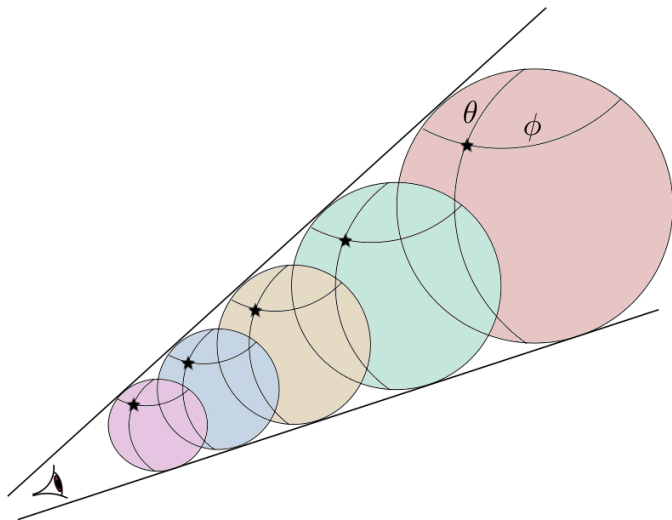


Motivations
○○○○○

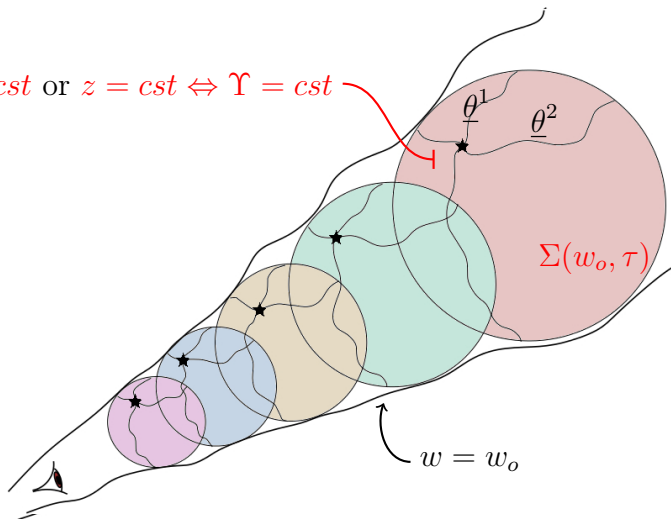
Relat. corr. with adapted coords.
○○●○○○○○○○○○○○○○○○○○○○○○○

Local universe inhomogeneity
○○○○○○○○○○○○○○○○○○○○○○○○○○○○

Conclusions
○○

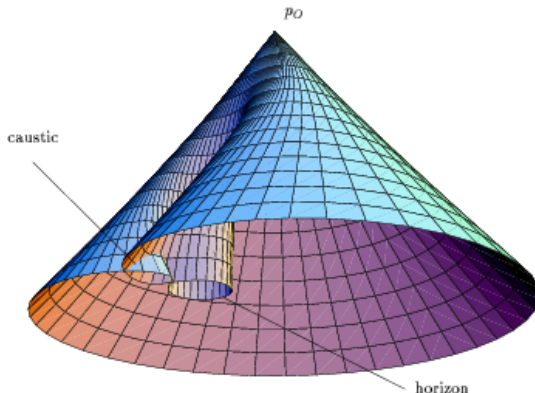


$$\tau = cst \text{ or } z = cst \Leftrightarrow \Upsilon = cst$$



NO CAUSTICS !

Way to generalization?



Geodesic light-cone coordinates

$$ds_{\text{GLC}}^2 = \Upsilon^2 dw^2 - 2\Upsilon d\omega d\tau + \gamma_{ab}(d\theta^a - U^a d\omega)(d\theta^b - U^b d\omega)$$

(6 arbitrary functions : $\Upsilon, U^a, \gamma_{ab}$)

Properties :

w is a **null coordinate**, $\partial_\mu \tau$ defines a **geodesic flow** (from $g_{GLC}^{\tau\tau} = -1$),
photons travel at $(w, \theta^a) = \overrightarrow{cst} \perp$ to $\Sigma(w, z)$.

Interpretation :

Υ is like an **inhomogeneous scale factor** (lapse function), U^a is a **shift-vector** and γ_{ab} the **metric inside the 2-sphere** $\Sigma(\tau, w)$.

FLRW :

$$w = \eta + r, \quad \tau = t, \quad (\theta^1, \theta^2) = (\theta, \phi),$$

$$\Upsilon = a(t), \quad U^a = 0, \quad \gamma_{ab} = a^2 r^2 \text{diag}(1, \sin^2 \theta).$$

Direct simplifications

$$ds_{GLC}^2 = \Upsilon^2 d\omega^2 - 2\Upsilon d\omega d\tau + \gamma_{ab}(d\theta^a - U^a d\omega)(d\theta^b - U^b d\omega)$$

⇒ **Redshift perturbation** (cf. Giuseppe's talk) :

$$(1 + z_s) = \frac{(k^\mu u_\mu)_s}{(k^\mu u_\mu)_o} = \frac{(\partial^\mu w \partial_\mu \tau)_s}{(\partial^\mu w \partial_\mu \tau)_o} = \frac{\Upsilon(w_o, \tau_o, \underline{\theta}^a)}{\Upsilon(w_o, \tau_s, \underline{\theta}^a)} \equiv \frac{\Upsilon_o}{\Upsilon_s}$$

where $u_\mu = -\partial_\mu \tau$ is the **peculiar velocity** of the **comoving** observer/source and $k_\mu = \partial_\mu w$ is the **photon momentum**.

⇒ **(exact) Angular distance** (with homogeneous observer neighborhood) :

$$d_A = \gamma^{1/4} (\sin \theta^1)^{-1/2} \quad \text{with} \quad \gamma \equiv \det(\gamma_{ab}) = |\det(g_{GLC})|/\Upsilon^2$$

which, combined with redshift, gives the **distance-redshift relation**.

Hubble diagram

Magnitude :

$$m = -2.5 \log_{10} \left(\frac{\Phi}{\Phi_{\text{ref}}} \right)$$

Flux :

$$\Phi = \frac{L}{4\pi d_L^2}$$

Absolute Mag. :

$$M = -2.5 \log_{10} \left(\frac{\Phi(10\text{pc})}{\Phi_{\text{ref}}(\text{pc})} \right)$$

Distance Modulus :

$$\mu = m - M = 5 \log_{10}(d_L) + cst$$

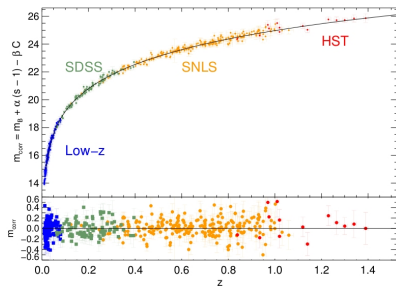
Two assumptions in SMC :

- GR valid on all scales,
- Isotropy + Homogeneity,

⇒ FLRW model.

Luminosity Distance (for $K = 0$) :

$$d_L^{FLRW}(z) = \frac{1+z}{H_0} \int_0^z \frac{dz'}{[\Omega_{\Lambda 0} + \Omega_{m0}(1+z')^3]^{1/2}}$$



Distance-redshift relation at $\mathcal{O}(2)$

The GLC metric allows to compute the $d_L(z)$ relation to $\mathcal{O}(2)$ in NG :

$$ds_{NG}^2 = a^2(\eta) \left(-(1 + 2\Phi) d\eta^2 + (1 - 2\Psi) (dr^2 + \gamma_{ab}^{(0)} d\theta^a d\theta^b) \right)$$

with $\gamma_{ab}^{(0)} = r^2 \text{diag} (1, \sin^2 \theta)$, and $\Phi = \psi + \frac{1}{2}\phi^{(2)}$, $\Psi = \psi + \frac{1}{2}\psi^{(2)}$ (Bardeen).

$$\psi^{(2)}, \phi^{(2)} \propto \nabla^{-2}(\partial_i \psi \partial^i \psi) , \quad \partial_i \psi \partial^i \psi \quad (\text{cf. Bartolo, Matarrese, Riotto, 2005})$$

FULL transformation GLC \leftrightarrow NG **at second order** in PT :

$$(\tau, w, \tilde{\theta}^1, \tilde{\theta}^2) = f(\eta, r, \theta, \phi)$$

$$\Downarrow$$

$$(\Upsilon, U^a, \gamma^{ab}) = f(\psi, \psi^{(2)}, \phi^{(2)})$$

$$\Downarrow$$

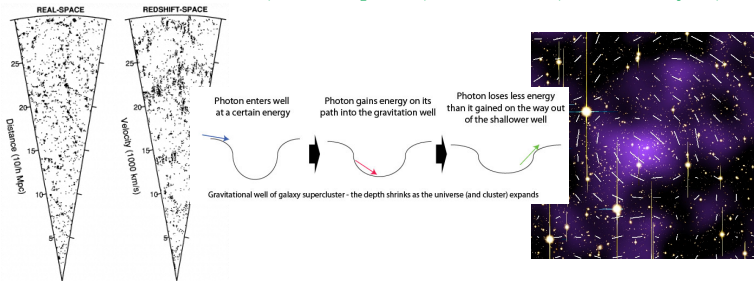
$$d_L = (1+z)^2 \gamma^{1/4} \left(\sin \tilde{\theta}^1 \right)^{-1/2} \text{ up to } \mathcal{O}(2) :$$

$$d_L(z_s, \theta^a) = d_L^{FLRW}(z_s) \left(1 + \delta_S^{(1)}(z_s, \theta^a) + \delta_S^{(2)}(z_s, \theta^a) \right)$$

Compute the **distance-redshift relation** at $\mathcal{O}(2)$ in perturbations (from the Newtonian gauge, 1104.1167, 1209.4326, 1506.02003) :

$$d_L(z_s, \underline{\theta}^a) = d_L^{FLRW}(z_s) \left(1 + \delta_S^{(1)}(z_s, \underline{\theta}^a) + \delta_S^{(2)}(z_s, \underline{\theta}^a) \right)$$

Contributors : G. Veneziano, M. Gasperini, G. Marozzi, I. Ben-Dayan, G. Fanizza



Qualitative agreement with O. Umeh, C. Clarkson and R. Maarten '14, Bonvin, Clarkson, Durrer, Maartens, Umeh '15, Kaiser, Peacock '15.

Detailed comparison? Difficult task. (see Yoo, Scaccabarozzi '16)

At $\mathcal{O}(1)$:

$$\delta_S^{(1)}(z_s, \theta^a) \sim \text{SW} + \text{ISW} + \text{Doppler} - \left(\psi_s^{(1)} + \int_{\eta_+}^{\eta_-} dx \psi \right) - \text{Lensing}^{(1)}$$

$$\text{Lensing}^{(1)} = \frac{1}{2} \nabla_a \theta^{a(1)} = \int_{\eta_s^{(0)}}^{\eta_o} \frac{d\eta}{\Delta\eta} \frac{\eta - \eta_s^{(0)}}{\eta_o - \eta} \Delta_2 \psi(\eta, \eta_o - \eta, \bar{\theta}^a)$$

$$\text{Doppler} = \left(1 - \frac{1}{\mathcal{H}_s \Delta\eta} \right) (\mathbf{v}_o - \mathbf{v}_s) \cdot \hat{n} \quad , \quad \mathbf{v} \equiv \int_{\eta_{\text{in}}}^{\eta} d\eta' \frac{a(\eta')}{a(\eta)} \nabla \psi(\eta', r, \theta^a)$$

At $\mathcal{O}(2)$, full calculation :

- Dominant terms : $(\text{Doppler})^2$, $(\text{Lensing})^2$!!!
- Combinations of $\mathcal{O}(1)$ -terms : ψ_s^2 , $([\text{I}]\text{SW})^2$, $[\text{I}]\text{SW} \times \text{Doppler}$, $(\psi_s, \int_{\eta_+}^{\eta_-} dx \psi) \times (\text{Lensing}, [\text{I}]\text{SW}, \text{Doppler}) \dots$
- Genuine $\mathcal{O}(2)$ -terms : $\psi_s^{(2)}$, $\text{Lensing}^{(2)} = \frac{1}{2} \nabla_a \theta^{a(2)}$, $Q_s^{(2)} \dots$
- A LOT of other contributions : New integrated effects, Angle deformations, Redshift perturbations (\subset transverse peculiar velocity), Lens-Lens coupling, corrections to Born approximation, ... See 1209.4326, also Umeh 1402.1933.

The whole second order... (up to some observer terms)

4.2. DETAILED EXPRESSION FOR $D_L(Z, \theta^A)$

$$\begin{aligned} \delta_{\text{path}}^{(2)} = & \Xi_* \left\{ -\frac{1}{4} (\phi^{(2)} - \psi^{(2)}) + \frac{1}{4} (\psi^{(2)} - \psi^{(2)}) + \frac{1}{2} (\psi_* - \psi_*)^2 - \psi_* J_*^{(1)} \right. \\ & + (\psi_* - \psi_* - J_*^{(1)}) \partial_\tau Q|_x + \frac{1}{4} (\gamma_0^A) \partial_\tau Q \partial_\tau Q + Q_* (-|\partial_\tau^2 Q|_x + |\partial_\tau \psi|_x) + \frac{1}{H_*} (\psi_* + |\partial_\tau Q|_x) |\partial_\tau \psi|_x \\ & - \frac{1}{2} \int_{\eta_*}^{\eta_*^+} d\eta' \frac{a(\eta')}{a(\eta_*)} \partial_\tau \left[\phi^{(2)} - \psi^{(2)} \right] (\eta', \Delta\eta, \tilde{\theta}^*) + \frac{1}{2} \int_{\eta_*}^{\eta_*^+} d\eta' \frac{a(\eta')}{a(\eta_*)} \partial_\tau \left[\phi^{(2)} - \psi^{(2)} \right] (\eta', 0, \tilde{\theta}^*) \\ & + \frac{1}{4} \int_{\eta_*^+}^{\eta_*^+} dx \partial_\tau \left[\hat{\phi}^{(2)} + \hat{\psi}^{(2)} + 4\hat{\psi} \partial_\tau Q + \gamma_0^A \partial_\tau Q \partial_\tau Q \right] (\eta_*^{(0)+}, x, \tilde{\theta}^*) \\ & - \frac{1}{2} \partial_\tau (\psi_* + \partial_\tau Q_*) \left(\int_{\eta_*^+}^{\eta_*^+} dx \left[\gamma_0^A \partial_\tau Q \right] (\eta_*^{(0)+}, x, \tilde{\theta}^*) \right) \Big\} \\ & - \frac{1}{2} \psi_*^{(2)} - \frac{1}{2} \psi_*^2 - K_2 + \psi_* J_*^{(1)} + \frac{1}{2} (J_*^{(1)})^2 + (J_*^{(1)} - \psi_*) \frac{Q_*}{\Delta\eta} - \frac{1}{H_* \Delta\eta} \left(1 - \frac{H_*}{H_*^2} \right) \frac{1}{2} (\psi_* + |\partial_\tau Q|_x)^2 \\ & - \frac{2}{H_* \Delta\eta} \psi_* (\psi_* + |\partial_\tau Q|_x) + \frac{1}{2} \partial_\tau \left(\psi_* + J_*^{(1)} + \frac{Q_*}{\Delta\eta} \right) \left(\int_{\eta_*^+}^{\eta_*^+} dx \left[\gamma_0^A \partial_\tau Q \right] (\eta_*^{(0)+}, x, \tilde{\theta}^*) \right) \\ & + \frac{1}{4} \partial_\tau Q_* \partial_\tau \left(\int_{\eta_*^+}^{\eta_*^+} dx \left[\gamma_0^A \partial_\tau Q \right] (\eta_*^{(0)+}, x, \tilde{\theta}^*) \right) \\ & + \frac{1}{16} \partial_\tau \left(\int_{\eta_*^+}^{\eta_*^+} dx \left[\gamma_0^A \partial_\tau Q \right] (\eta_*^{(0)+}, x, \tilde{\theta}^*) \right) \partial_\tau \left(\int_{\eta_*^+}^{\eta_*^+} dx \left[\gamma_0^A \partial_\tau Q \right] (\eta_*^{(0)+}, x, \tilde{\theta}^*) \right) \\ & - \frac{1}{4\Delta\eta} \int_{\eta_*^+}^{\eta_*^+} dx \left[\hat{\phi}^{(2)} + \hat{\psi}^{(2)} + 4\hat{\psi} \partial_\tau Q + \gamma_0^A \partial_\tau Q \partial_\tau Q \right] (\eta_*^{(0)+}, x, \tilde{\theta}^*) \\ & + \frac{1}{H_*} (\psi_* + |\partial_\tau Q|_x) \left\{ -|\partial_\tau \psi|_x + |\partial_\tau \psi|_x + \frac{1}{\Delta\eta^2} \int_{\eta_*^+}^{\eta_*^+} d\eta' \Delta\eta \psi(\eta', \eta_* - \eta', \tilde{\theta}^*) \right\} \\ & + Q_* \left\{ |\partial_\tau \psi|_x + \partial_\tau \left(\int_{\eta_*^+}^{\eta_*^+} dx \frac{1}{(\eta_*^{(0)+} - x)^2} d\eta' \Delta\eta \psi(\eta_*^{(0)+}, y, \tilde{\theta}^*) \right) \right\} \\ & + \frac{1}{2\Delta\eta^2} \int_{\eta_*^+}^{\eta_*^+} d\eta' \Delta\eta \psi(\eta', \eta_* - \eta', \tilde{\theta}^*) \Big\} + \frac{1}{16 \sin^2 \theta} \left(\int_{\eta_*^+}^{\eta_*^+} dx \left[\gamma_0^A \partial_\tau Q \right] (\eta_*^{(0)+}, x, \tilde{\theta}^*) \right)^2, \quad (4.67) \end{aligned}$$

$$\begin{aligned} \delta_{\text{path}}^{(2)} = & \frac{\Xi_*}{2} \left\{ (|\partial_\tau P|_x - |\partial_\tau P|_x)^2 + (\gamma_0^A) \partial_\tau P_* \partial_\tau P_* - \lim_{\eta \rightarrow \eta_*} \left[\gamma_0^A \partial_\tau P \partial_\tau P \right] \right. \\ & - \frac{2}{H_*} (|\partial_\tau P|_x - |\partial_\tau P|_x) (H_* |\partial_\tau P|_x + |\partial_\tau^2 P|_x) \\ & - \int_{\eta_*}^{\eta_*^+} d\eta' \frac{a(\eta')}{a(\eta_*)} \partial_\tau \left\{ (|\partial_\tau P|_x)^2 + \gamma_0^A \partial_\tau P \partial_\tau P \right\} (\eta', \Delta\eta, \tilde{\theta}^*) \\ & + \int_{\eta_*}^{\eta_*^+} d\eta' \frac{a(\eta')}{a(\eta_*)} \partial_\tau \left\{ (|\partial_\tau P|_x)^2 + \gamma_0^A \partial_\tau P \partial_\tau P \right\} (\eta', 0, \tilde{\theta}^*) \Big\} - \frac{1}{2H_* \Delta\eta} \left(1 - \frac{H_*}{H_*^2} \right) (|\partial_\tau P|_x - |\partial_\tau P|_x)^2, \quad (4.68) \end{aligned}$$

$$\begin{aligned} \delta_{\text{meas}}^{(2)} = & \Xi_* \left\{ 2(\psi_* - \psi_* + \partial_\tau Q_* - \frac{Q_*}{\Delta\eta}) |\partial_\tau P|_x - (|\partial_\tau P|_x - |\partial_\tau P|_x) \left(\frac{1}{H_*} |\partial_\tau \psi|_x - J_*^{(1)} \right) \right. \\ & - (\gamma_0^A) \partial_\tau Q_* \partial_\tau P_* + \frac{1}{H_*} (\psi_* + |\partial_\tau Q|_x) |\partial_\tau^2 P|_x + Q_* |\partial_\tau^2 P|_x \\ & + \frac{1}{2} \partial_\tau (|\partial_\tau P|_x - |\partial_\tau P|_x) \left(\int_{\eta_*^+}^{\eta_*^+} dx \left[\gamma_0^A \partial_\tau Q \right] (\eta_*^{(0)+}, x, \tilde{\theta}^*) \right) \Big\} \\ & + \frac{1}{\Delta\eta} (|\partial_\tau P|_x - |\partial_\tau P|_x) \left\{ \frac{1}{H_*} \left(1 - \frac{H_*}{H_*^2} \right) (\psi_* + |\partial_\tau Q|_x) + \frac{2}{H_*} \psi_* + Q_* \right\} \\ & + \frac{1}{H_*} (|\partial_\tau P|_x - |\partial_\tau P|_x) \left\{ |\partial_\tau \psi|_x - |\partial_\tau \psi|_x - \frac{1}{\Delta\eta^2} \int_{\eta_*^+}^{\eta_*^+} d\eta' \Delta\eta \psi(\eta', \eta_* - \eta', \tilde{\theta}^*) \right\}. \quad (4.69) \end{aligned}$$



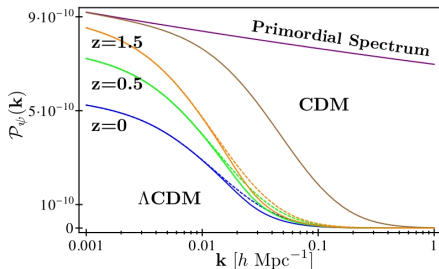
Stochastic average of inhomogeneous realizations

Inhomogeneities :

$$\psi(\eta, \vec{x}) = \int \frac{d^3k}{(2\pi)^{3/2}} e^{i\vec{k} \cdot \vec{x}} \psi_k(\eta) E(\vec{k})$$

with E a unit R.V. which is
homogeneous ($E^*(\vec{k}) = E(-\vec{k})$) and
gaussian ($\overline{E(\vec{k})} = 0$, $\overline{E(\vec{k}_1)E(\vec{k}_2)} = \delta(\vec{k}_1 + \vec{k}_2)$).

Spectrum : $|\psi_k(\eta)|^2 = 2\pi^2 \mathcal{P}_\psi(k)/k^3$



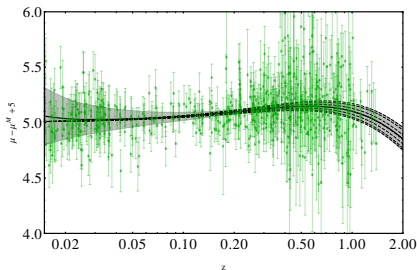
Light-cone average is combined with a stochastic average. In **CDM** :

$$\overline{\langle d_L \rangle} = \int_0^\infty \frac{dk}{k} \mathcal{P}_\psi(k) C(k\Delta\eta)$$

We do the same \forall terms in $\overline{\langle \delta_S^{(1)} \rangle}$ and $\overline{\langle \delta_S^{(2)} \rangle}$ in **LambdaCDM**... with approximations.

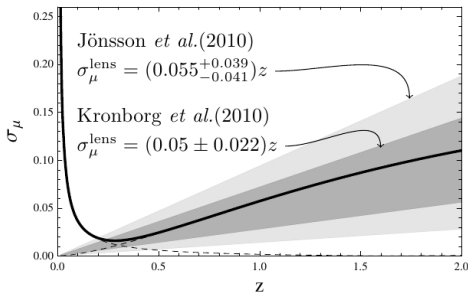
Kaiser & Peacock 2015 for precise discussion on 'directional' / 'source' averaging.

The **averaged modulus** $\overline{\langle \mu \rangle}$ depends on $\overline{\langle (\Phi_1/\Phi_0)^2 \rangle}$ while the **standard deviation** $\sigma_\mu = \sqrt{\overline{\langle \mu^2 \rangle} - \overline{\langle \mu \rangle}^2} = 2.5(\log_{10} e) \sqrt{\overline{\langle (\Phi_1/\Phi_0)^2 \rangle}}$ with $\overline{\langle (\Phi_1/\Phi_0)^2 \rangle} \sim \overline{\langle (\text{Doppler})^2 \rangle} + \overline{\langle (\text{Lensing}^{(1)})^2 \rangle}$



With the Union 2 dataset :

- small z : **Velocities** explain quite well the scatter.
- large z : **Lensing** is too weak to explain data's scatter ($\sim \% \Omega_{\Lambda 0}$).

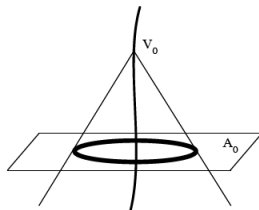
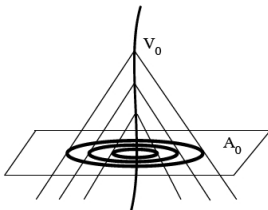
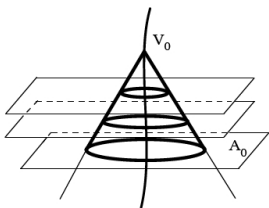


- The total effect is well approximated by **Doppler** ($z \leq 0.2$) + **Lensing** ($z > 0.3$),
- **Lensing** prediction is in great agreement with experiments so far !

Cf. Ben-Dayan 2014, 1401.7973 for effect on H_0 .

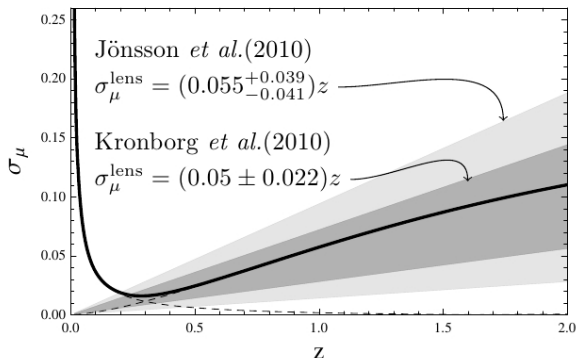
Simplify averages on the past lightcone (1207.1286, 1302.0740) :

$$\begin{aligned}\langle S \rangle_{w_o, \tau_s} &= \frac{\int_{\Sigma} d^4x \sqrt{-g} \delta_D(w - w_o) \delta_D(\tau - \tau_s) |\partial_{\mu} \tau \partial^{\mu} w| S(\tau, w, \underline{\theta}^a)}{\int_{\Sigma} d^4x \sqrt{-g} \delta_D(w - w_o) \delta_D(\tau - \tau_s) |\partial_{\mu} \tau \partial^{\mu} w|} \\ &= \frac{\int d^2 \underline{\theta} \sqrt{\gamma(w_o, \tau_s, \underline{\theta}^a)} S(w_o, \tau_s, \underline{\theta}^a)}{\int d^2 \underline{\theta} \sqrt{\gamma(w_o, \tau_s, \underline{\theta}^a)}}\end{aligned}$$



$$V_0 \sim w_0 \quad , \quad A_0 \sim \tau_s$$

Estimate the effect of **large scale structure** on the **Hubble diagram** :
average and dispersion of the distance modulus ([my thesis](#), 1309.6542, and
 [\$d_L\$ references above](#)).



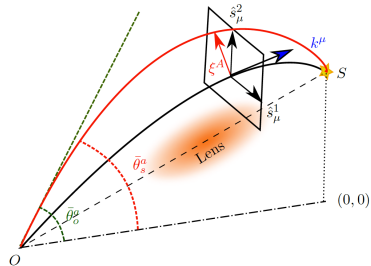
Measurements to confirm this prediction?

Other applications of GLC

Amplification matrix $((\dots)^\bullet \equiv \partial_\tau(\dots))$:

$$\begin{aligned} \mathcal{A}_B^A(\lambda_s, \lambda_o) &= \frac{s_a^A(\lambda_s) [2u_\tau(\dot{\gamma}_{ab})^{-1}]_o s_b^B(\lambda_o)}{\bar{d}_A(\lambda_s)} \\ &= \begin{pmatrix} 1 - \kappa - \hat{\gamma}_1 & -\hat{\gamma}_2 + \hat{\omega} \\ -\hat{\gamma}_2 - \hat{\omega} & 1 - \kappa + \hat{\gamma}_1 \end{pmatrix} \end{aligned}$$

Fanizza, Nugier 2014, 1408.1604



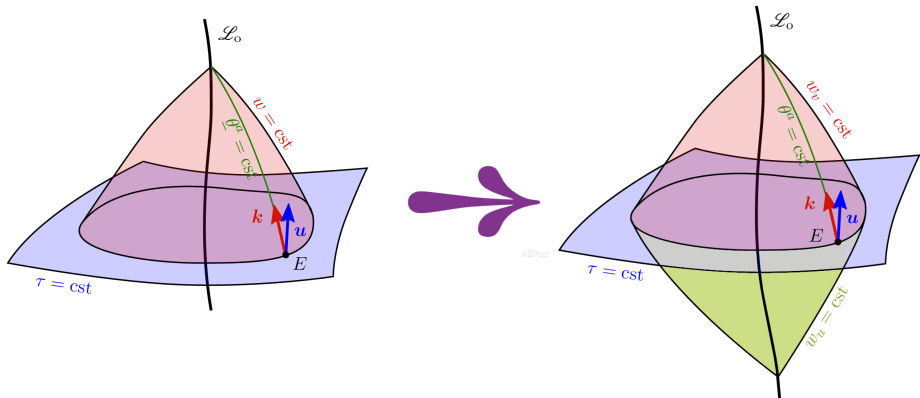
The **angular distance** and **lensing quantities** become :

$$d_A \propto (\gamma \gamma_o)^{1/4} \quad , \quad \hat{\mu} = (\det \mathcal{A})^{-1} = \left(\frac{\bar{d}_A}{d_A} \right)^2 \quad ,$$

involving $\bar{d}_A = a(\tau)r$ with $r = w - \int a^{-1}(\tau) d\tau$ measured from the observer,

$$\left\{ \begin{array}{c} (1 - \kappa)^2 + \hat{\omega}^2 \\ \hat{\gamma}_1^2 + \hat{\gamma}_2^2 \end{array} \right\} = \left(\frac{u_{\tau_o}}{\bar{d}_A} \right)^2 \left\{ \left[\frac{\gamma \dot{\gamma}_{ab} \gamma^{bc} \dot{\gamma}_{cd}}{(\det^{ab} \dot{\gamma}_{ab})^2} \right]_o \gamma \gamma^{ad} \pm 2 \frac{\sqrt{\gamma \gamma_o}}{(\det^{ab} \dot{\gamma}_{ab})_o} \right\}$$

Turning TIME into FUTURE NULL coordinate!



$$x^\mu \equiv (\tau, w, \underline{\theta}^a)$$

$$y^\mu \equiv (w_u, w_v, \theta^a)$$

“(Geodesic \rightarrow Double) Light-Cone coordinates”

Nugier 2016, 1606.08296

$$y^\mu \equiv (w_u, w_v, \theta^a) \quad \rightarrow \quad g_{\mu\nu}^{\text{DLC}}(y) = \frac{\partial x^\alpha}{\partial y^\mu} \frac{\partial x^\beta}{\partial y^\nu} g_{\alpha\beta}^{\text{GLC}}(x) \quad \leftarrow \quad x^\mu \equiv (\tau, w, \underline{\theta}^a)$$

- $w = w_v \Rightarrow \partial w / \partial w_v = 1$
- w_u independent from $w_v \Rightarrow \partial w / \partial w_u = 0$
- in GLC $\underline{\theta}^a$ is independent from $w \Rightarrow \partial \underline{\theta}^a / \partial w_v = 0$
- light rays independent from $w_u \Rightarrow \partial \theta^a / \partial w_u = 0$.

$$g_{\mu\nu}^{\text{DLC}} = \begin{pmatrix} 0 & \textcolor{blue}{g_{w_u w_v}^{\text{DLC}}} & \vec{0} \\ \textcolor{blue}{g_{w_u w_v}^{\text{DLC}}} & \textcolor{red}{g_{w_v w_v}^{\text{DLC}}} & g_{w_v a}^{\text{DLC}} \\ \vec{0}^T & (g_{w_v w_v}^{\text{DLC}})^T & g_{ab}^{\text{DLC}} \end{pmatrix} \quad \text{with} \quad \begin{cases} \textcolor{blue}{g_{w_u w_v}^{\text{DLC}}} = -\Upsilon \frac{\partial \tau}{\partial w_u} \quad , \\ \textcolor{red}{g_{w_v w_v}^{\text{DLC}}} = (\Upsilon^2 + U^2) - 2\Upsilon \frac{\partial \tau}{\partial w_v} \end{cases}$$

- $\theta^a = \underline{\theta}^a$ (residual gauge freedom on $\Sigma(w_u, w_v)$) $\Rightarrow \partial \underline{\theta}^a / \partial \theta^b \equiv \delta_b^a$
- natural consequence $\Rightarrow \partial w / \partial \theta^a = 0$

$$g_{\text{DLC}}^{\mu\nu} = \begin{pmatrix} g_{\text{DLC}}^{w_u w_u} & -2/\tilde{\Upsilon}^2 & -2\tilde{U}^b/\tilde{\Upsilon}^2 \\ -2/\tilde{\Upsilon}^2 & 0 & \vec{0} \\ -2(\tilde{U}^a)^T/\tilde{\Upsilon}^2 & \vec{0}^T & \gamma^{ab} \end{pmatrix} \quad \text{from} \quad \left\{ \begin{array}{l} g_{ab}^{\text{DLC}} = \gamma_{ab} \quad , \\ g_{w_v a}^{\text{DLC}} = -U_a - \Upsilon \frac{\partial \tau}{\partial \theta^a} \equiv -\tilde{U}_a \end{array} \right.$$

Summary GLC/DLC

DLC = GLC for which we replace τ by a future null coordinate w_u !

$$ds_{\text{GLC}}^2 = \Upsilon^2 dw^2 - 2\Upsilon dw d\tau + \gamma_{ab} (d\theta^a - U^a dw) (d\theta^b - U^b dw)$$

↓

$$ds_{\text{DLC}}^2 = -\tilde{\Upsilon}^2 dw_u dw_v + \gamma_{ab} (d\theta^a - \tilde{U}^a dw_v) (d\theta^b - \tilde{U}^b dw_v)$$

$$\tilde{U}^a \equiv \gamma^{ab} \tilde{U}_b = U^a + \Upsilon \gamma^{ab} \frac{\partial \tau}{\partial \theta^b} \quad ,$$

$$\frac{\partial \tau}{\partial w_u} = \frac{\tilde{\Upsilon}^2}{2\Upsilon} \quad , \quad \frac{\partial \tau}{\partial w_v} = \frac{\Upsilon}{2} - \tilde{U}^a \frac{\partial \tau}{\partial \theta^a} + \frac{\Upsilon}{2} \gamma^{ab} \frac{\partial \tau}{\partial \theta^a} \frac{\partial \tau}{\partial \theta^b} \quad .$$

$$g_{\mu\nu}^{\text{GLC}} = \begin{pmatrix} 0 & -\Upsilon & \vec{0} \\ -\Upsilon & \Upsilon^2 + U^2 & -U_b \\ \vec{0}^T & -U_a^T & \gamma_{ab} \end{pmatrix} \quad , \quad g_{\text{GLC}}^{\mu\nu} = \begin{pmatrix} -1 & -\Upsilon^{-1} & -U^b/\Upsilon \\ -\Upsilon^{-1} & 0 & \vec{0} \\ -(U^a)^T/\Upsilon & \vec{0}^T & \gamma^{ab} \end{pmatrix} \quad ,$$

$$g_{\mu\nu}^{\text{DLC}} = \begin{pmatrix} 0 & -\tilde{\Upsilon}^2/2 & \vec{0} \\ -\tilde{\Upsilon}^2/2 & \tilde{U}^2 & -\tilde{U}_b \\ \vec{0}^T & -\tilde{U}_a^T & \gamma_{ab} \end{pmatrix} \quad , \quad g_{\text{DLC}}^{\mu\nu} = \begin{pmatrix} 0 & -2/\tilde{\Upsilon}^2 & -2\tilde{U}^b/\tilde{\Upsilon}^2 \\ -2/\tilde{\Upsilon}^2 & 0 & \vec{0} \\ -2(\tilde{U}^a)^T/\tilde{\Upsilon}^2 & \vec{0}^T & \gamma^{ab} \end{pmatrix} \quad .$$

DLC = double-null coordinates !

Line element in the **double-null coordinates** :

$$ds^2 = e^\lambda \eta_{AB} dw^A dw^B + g_{ab} (d\theta^a + s^a_A dw^A) (d\theta^b + s^b_B dw^B)$$

So we get back DLC coordinates by taking :

$$\begin{aligned} dx^0 &= dw_u \quad , \quad dx^1 = dw_v \quad , \quad dx^a = s^a_{w_u} dw_u + (s^a_{w_v} + \tilde{U}^a) dw_v + d\theta^a \\ \lambda &= \ln \left(\tilde{\Upsilon}^2 / 2 \right) \quad , \quad s^a_{w_u} = 0 \quad , \quad s^a_{w_v} = -\tilde{U}^a \quad \text{(gauge fixing)} \end{aligned}$$

$\Rightarrow \tilde{U}^a$ is a **shift vector** in the (2+2) decomposition.

They are **equivalent to the double-null coordinates** of *Brady, Droz, Israel and Morsink 1995* after a gauge fixing !

Probing the local homogeneity with standard candles

Collaboration with Hsu-Wen Chiang (蔣序文),
Enea Romano, Pisin Chen (陳丕榮).

Motivations

- Estimate how **standard candles** can probe the **density contrast**.
- Investigate on H_0 as *Riess 2016* re-evaluates $H_0 = 73.24 \pm 1.74 \text{ km s}^{-1} \text{ Mpc}^{-1}$, raising the **tension to 3.4 σ** against $66.93 \pm 0.62 \text{ km s}^{-1} \text{ Mpc}^{-1}$ from Planck.
- Isotropic inhomogeneity extending very far should not exist, but anisotropic inhomogeneity may. *Keenan, Barger, Cowie '13* find a super-void extending to $z \sim 0.07$ ($\sim 300 h_{70}^{-1} \text{ Mpc}$).
- We know that being inside an underdense region may alleviate H_0 tension (see *Ben-Dayan, Durrer, Marozzi and Schwarz, 2014* and *Romano 2016*).

Method

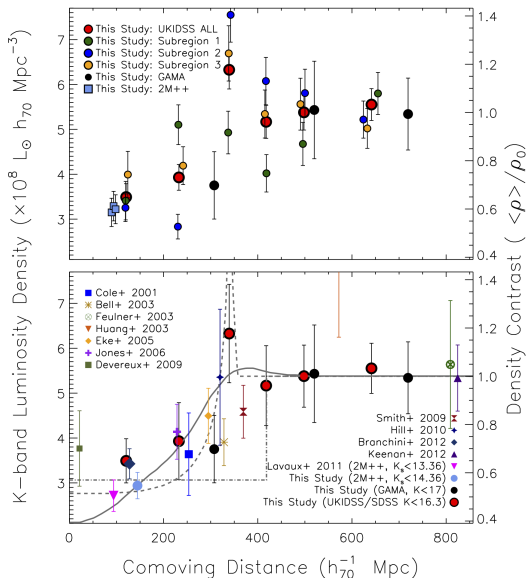
Model independent fit of luminosity distance observations (standard candles)

+ **Inversion** based on LTB to reconstruct the local radial density profile)
assuming Planck background, along two different directions of the sky.

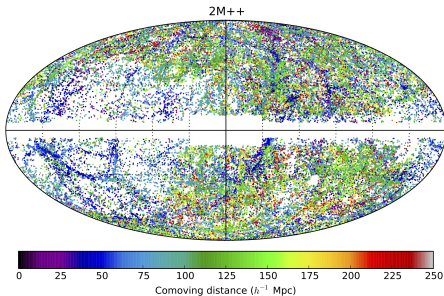
Comparison with : density maps obtained from luminosity density, in particular [Keenan et al. 2013](#) and the 2M++ galaxy catalogue.

Remark : See estimation of cosmic variance on H_0 in [Ben-Dayan, Durrer, Marozzi and Schwarz, '14](#).

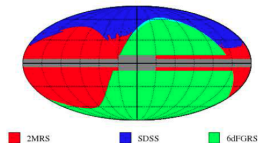
Keenan et al 2013, Figure 11



2M++ (Lavaux & Hudson 2011, Carrick *et al.* 2015)



Redshifts are from 2MRS, SDSS-DR7, and 6dFGRS.



Peculiar velocities are obtained from the galaxy density :

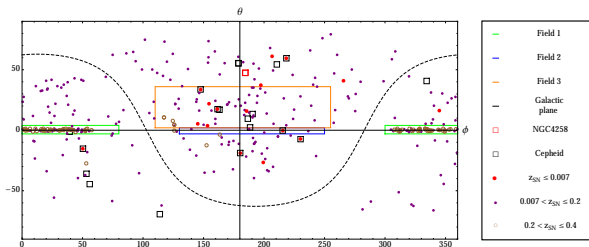
$$\vec{v}(\vec{r}) = \frac{\beta^*}{4\pi} \int_0^{R_{\max}} d^3\vec{r}' \delta_g^*(\vec{r}') \frac{\vec{r}'}{r'^3} \quad , \quad \bar{z} = z_{\text{obs}} - \vec{v} \cdot \vec{n}$$

where $\beta^* = 0.43$ is a best fit value and the upper limit of integration is the depth of the survey $R_{\max} = 200 h^{-1}\text{Mpc}$, i.e. $z = 0.067$.

\Rightarrow limited to **200 Mpc + an external bulk flow** (that we remove).

Data

Cepheids are from *Riess 2016* (z_{host} from NED) and **SNe Ia** from UNION 2.1 (with $z < 0.2$ or 0.4 and positions from SIMBAD), corrected to Riess H_0 .



Velocity dispersion : 250 km s^{-1} for SNe, $0, 40, 250 \text{ km s}^{-1}$ for Cepheids.
Implies a change in μ by $\Delta\mu_{\text{v.d.}} \approx \frac{5}{\log 10} \frac{\Delta v}{cz}$.

Field N ^o	ICRS coordinates (deg)		Number of SNe		Cepheids-hosting galaxies of Riess
	R.A.	Dec.	$z_{\text{max}} = 0.2$	$z_{\text{max}} = 0.4$	
1	$[300, 360] \cup [0, 80]$	$[-3, 4]$	69	144	1
2	$[130, 250]$	$[-3, 2]$	4+1	4+1	1
3	$[110, 255]$	$[2, 36]$	47+2	52+2	6
/	Whole Sky		288	372	20

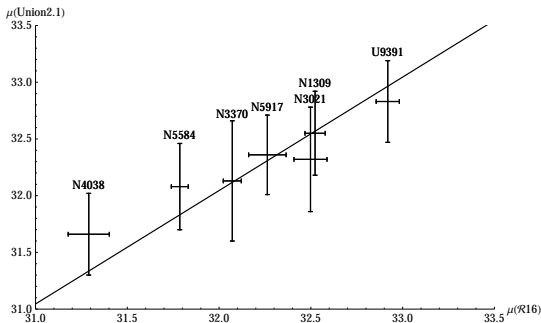
Initial rescaling

At small z :

$$\mu \equiv m - M = 25 - 5 \log_{10} H_0^{\text{loc}} + 5 \log_{10} (H_0^{\text{loc}} D_L) \approx 25 - 5 \log_{10} H_0^{\text{loc}} + 5 \log_{10} cz$$

where H_0^{loc} is the local Hubble parameter.

$$\Rightarrow \mu(\mathcal{R}16) = \mu(\text{Union 2.1}) - 5 \log_{10} \left(\frac{73.24}{70} \right)$$



7 host galaxies common to $\mathcal{R}16$ Cepheids and UNION 2.1 SNe

1D Fitting

Fits of the distance modulus data $(z_i, \mu_i, \Delta\mu_i)$ by minimizing χ^2 of the deviation from a homogeneous model :

$$\chi^2 = \sum_i \left(\frac{f(z_i) - (\mu_i - \mu^{\text{Planck}}(z_i))}{\Delta\mu_i} \right)^2, \quad f(z) = (\mu^{\text{obs}} - \mu^{\text{Planck}})(z)$$

where $\mu^{\text{Planck}}(z)$ is the Λ CDM theoretical value of distance modulus at z .

Model independent by decomposing the fitting function $f(z)$ wrt a set of *radial basis functions* (RBFs NN) :

$$f(z) = w_0 + w_{-1} z + \sum_{m=1}^{N_{\text{NL}}} w_m \Phi(|z - p_m|)$$

where Φ are chosen to be $\Phi(r) = r^3$ (N_{NL} RBFs), p_m are the **non-linear parameters** or “centers” of the RBFs, w_m the linear parameters, w_0 (intercept) and/or w_{-1} (slope) parameters.

Best fit and confidence bands

Linear parameters $\mathbf{w} \equiv (w_{-1}, \dots, w_{N_{\text{NL}}})$: we use the simple Moore-Penrose pseudo-inverse method.

Non-linear parameters $\mathbf{p} \equiv (p_1, \dots, p_{N_{\text{NL}}})$: we use a Monte Carlo (MC) random sampling method and a LO algorithm (Gauss-Newton).

To speed up the MC process and fill up confidence band : we use a Monte Carlo Markov Chain (MCMC) algorithm to explore the non-linear parameter space (see paper for illustration).

A fitting model is classified by a set of parameters $(N_0, N_{-1}, N_{\text{NL}})$.

We use a F-test to determine the **best model parameters**.

Density contrast (Romano, Chiang and Chen, 2013)

LTB metric and EFEs :

$$ds^2 = dt^2 - a^2 \left[\left(1 + \frac{a_{,r} r}{a} \right)^2 \frac{dr^2}{1 - k(r)r^2} + r^2 d\Omega_2^2 \right]$$

$$\left(\frac{\dot{a}}{a} \right)^2 = -\frac{k(r)}{a^2} + \frac{\rho_0(r)}{3a^3} \quad , \quad \rho(t, r) = \frac{(\rho_0 r^3)_{,r}}{3a^2 r^2 (ar)_{,r}} \quad ,$$

Solution of the EFEs can be expressed in conformal time $\eta = \int^t dt' / a(t', r)$:

$$a(\eta, r) = \frac{\rho_0}{6k(r)} \left[1 - \cos \left(\sqrt{k(r)} \eta \right) \right]$$

$$t(\eta, r) = \frac{\rho_0}{6k(r)} \left[\eta - \frac{1}{\sqrt{k(r)}} \sin \left(\sqrt{k(r)} \eta \right) \right] + (t_b(r) \equiv 0)$$

$$\Rightarrow D_L(z) = (1 + z)^2 r(z) a(\eta(z), r(z)) \quad ,$$

where $\eta(z)$ and $r(z)$ are the solutions of the radial ingoing null geodesic equations, and the redshift z is defined by $\frac{1+z_s}{1+z_o} = \exp \left(\partial_{t_s} \int_s^o \frac{dt}{dr} \right)$.

To obtain $r(z)$, $\eta(z)$ and $k(z)$, **the relation of D_L needs to be inverted and solved together with the radial null geodesic equations $\Rightarrow \rho(z, D_L(z))$.**

Inversion (Romano, Chiang and Chen, 2013), i.e. what we solve :

$$a(z=0) = a_0, \quad H_{\text{LTB}}(z=0) \equiv [a^{-1} \partial_t a](z=0) = H_0, \quad (\text{I.C.})$$

$$q_{\text{LTB}}(z=0) \equiv \left[-a (\partial_t a)^{-2} \partial_t \partial_t a \right] (z=0) = q_0, \quad r(z=0) = 0, \quad (\text{I.C.})$$

$$\frac{dk}{dz} = \frac{\sqrt{1-S^2}}{3(1+z)S} \frac{2k \tan(\tau/2) \mathcal{A}}{3 - \tau \csc(\tau)(2 + \cos(\tau))},$$

$$\frac{d\eta}{dz} = \frac{1}{(1+z)\sqrt{k}} \left(\csc(\tau) \mathcal{B} - \frac{\sqrt{1-S^2}}{3S} \mathcal{A} \right),$$

$$\frac{dr}{dz} = \frac{\sqrt{1-S^2}}{(1+z)\sqrt{k}} \left(\frac{\cos(\tau) + 3\tau \csc(\tau) - 4}{3 - \tau \csc(\tau)(2 + \cos(\tau))} \frac{\csc(\tau) \mathcal{A}}{3} + \tan(\tau/2) \right),$$

where we have defined

$$\tau \equiv \sqrt{k} \eta, \quad S \equiv \sqrt{k} r, \quad \mathcal{A} = 1 - \cos(\tau) + \mathcal{B}$$

$$\mathcal{B} = \frac{2}{S} \frac{(a_0 H_0)^{-3} (1+z) k^{3/2}}{1 - \tan(\tau/2) \sqrt{1-S^2}/S} \left(1 - \frac{1+2q_0}{4(1+q_0)^2} \right)^{-1} \frac{d}{dz} \left(\frac{H_0 D_{\text{L}}(z)}{(1+z)^2} \right).$$

The density is then given

$$\rho(z) = \rho(t(z), r(z)) = \frac{a^{-3} \rho_0}{1 + r \left(\partial_r \ln a|_\eta - \frac{\partial_t}{a \partial r} \partial_\eta \ln a|_r \right)}, \quad \rho_0 \equiv 3H_0^2 \left[1 - \frac{1+2q_0}{4} (1+q_0)^{-2} \right]$$

Density contrast :

$$\delta_C = f^{-1} \left(\frac{\rho_{\text{inv}}(D_L, z)}{\rho_{\text{inv}}(D_L^{\text{Planck}}, z)} - 1 \right), \quad f^{-1} = \Omega_{m0}^{-0.55}.$$

Full sky fitting

Applying peculiar velocity correction (PVC) from 2M++ and velocity dispersion (VD) of 250 km s^{-1} for SNe (Riess 2016 applies 250 km s^{-1} also for Cepheids).

250 km s^{-1} VD for Cepheids :

\Rightarrow Preferred model is **(1,0,0)** : $f(z) = \mu^{\text{obs}}(z) - \mu^{\text{Planck}}(z) = w_0$, i.e. homogeneous model with an apparent value of the Hubble parameter :

$$H_0^{\text{loc}} \equiv H_0^{\text{Planck}} 10^{-f(z=0)/5} = H_0^{\text{Planck}} 10^{-w_0/5} = 10^{-w_0/5} (66.93 \text{ km s}^{-1} \text{ Mpc}^{-1}).$$

We find : $H_0^{\text{loc}} = 73.06 \pm 1.61 \text{ (stat.) km s}^{-1} \text{ Mpc}^{-1}$, in good agreement with $73.24 \pm 1.61 \text{ (stat.)} \pm 0.66 \text{ (sys.) km s}^{-1} \text{ Mpc}^{-1}$ of Riess 2016 (we have $\chi_R^2 = 1.49$).

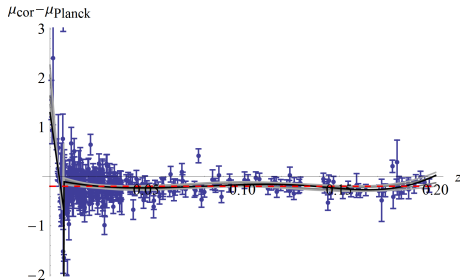
40 km s^{-1} VD for Cepheids :

(see Tully 2007)

Best fit is a (0, 1, 7) model!

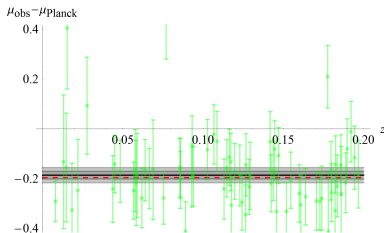
$$\chi_R^2 = 4.18$$

\Rightarrow there must be structure not accounted for by 2M++.



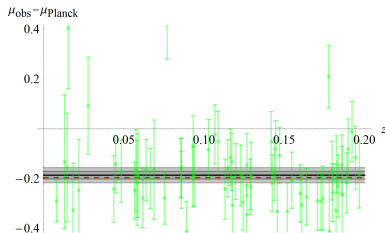
Directional fitting in F1

With PVC from 2M++ :



- best fit we get is from a simple $(1, 0, 0)$ model with $H_0^{\text{loc}} = 72.89 \pm 0.50 \text{ km s}^{-1} \text{ Mpc}^{-1}$ and $\chi_R^2 = 1.05$ (see figure),
- next best fit (Threshold < 33%) is given by a $(0, 1, 5)$ model with $\chi_R^2 = 0.88$.

Without PVC from 2M++ :



- best fit model is $(1, 0, 0)$ with $H_0^{\text{loc}} = 72.90 \pm 0.51 \text{ km s}^{-1} \text{ Mpc}^{-1}$ with F-test *Threshold* > 36% and $\chi_R^2 \sim 1.07$ (see figure),
- second best model is an inhomogeneous $(1, 1, 13)$ model with $\chi_R^2 \sim 0.59$ but low threshold.

Directional fitting in F3 with PVC

Applying **PVC** from 2M++ and a **velocity dispersion** (VD) of 250 km s⁻¹ for SNe Ia (host rotation), and no VD for Cepheids.

It is necessary to **remove some “outliers”** to have invertible fits.
We use a F-test *Threshold* around 95% to compare a given model with a constant fit model.

$z_{\max} = 0.2$			
χ_R^2	<i>Threshold</i> (%)	<i>Param.</i>	Removal
19.5	Not Preferred	76.40 ± 2.90	
1.59	81 ~ 100%	(0, 1, 6)	
5.92	95.8 ~ 100%	(0, 0, 0)	NGC 4536
2.06	90.7 ~ 95.7%	(0, 1, 3)	Same
2.05	73 ~ 100%	70.56 ± 0.93	+NGC 4424

$z_{\max} = 0.4$			
χ_R^2	<i>Threshold</i> (%)	<i>Param.</i>	Removal
17.9	Not Preferred	76.36 ± 2.75	
1.60	74 ~ 100%	(0, 1, 6)	
5.58	96.9 ~ 100%	(0, 0, 0)	NGC 4536
2.03	85 ~ 96.8%	(0, 1, 3)	Same
2.00	72 ~ 100%	70.65 ± 0.91	+NGC 4424

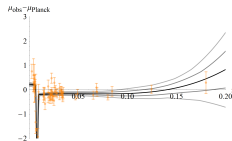
Directional fitting in F3 without PVC

We don't apply PVC since we want to see the whole contribution from SNe Ia and Cepheids.

Just apply a VD of 250 km s^{-1} for SNe Ia (host rotation).

$z_{\text{max}} = 0.2$			
χ_R^2	Threshold (%)	Param.	Removal
1.40	39 ~ 100	(0, 0, 5)	
3.45	97.5 ~ 100	(0, 0, 0)	NGC 4536
2.26	89 ~ 97.4	(1, 0, 1)	Same
2.88	99.5 ~ 100	(0, 0, 0)	+1999cl
1.55	94.1 ~ 99.4	(1, 0, 1)	Same
1.47	47 ~ 94.0	(0, 0, 2)	Same

$z_{\text{max}} = 0.4$			
χ_R^2	Threshold (%)	Param.	Removal
1.43	38 ~ 100	(0, 1, 5)	
3.31	92.6 ~ 100	(0, 0, 0)	NGC 4536
2.20	92.1 ~ 92.5	(0, 1, 2)	Same
2.80	96.3 ~ 100	(0, 0, 0)	+1999cl
1.96	89 ~ 96.2	(1, 0, 1)	Same
1.37	76 ~ 88	(0, 0, 4)	Same



Motivations
○○○○○

Relat. corr. with adapted coords.
○○○○○○○○○○○○○○○○○○○○○○○○○○○○○○○○

Local universe inhomogeneity
○○○○○○○○○○○○○○○○○○●○○○○○○○

Conclusions
○○

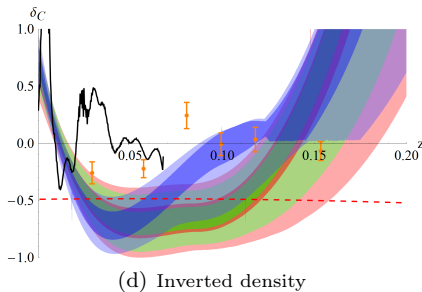
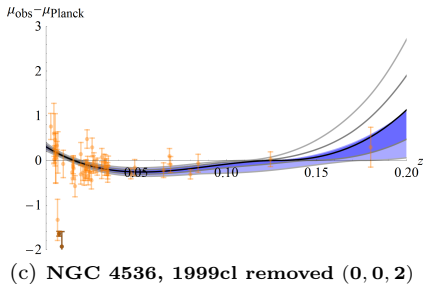
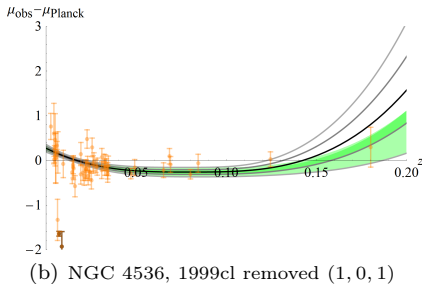
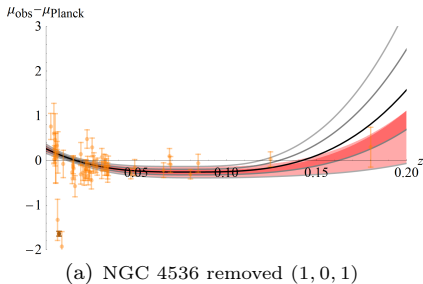


FIGURE: Distance modulus best fit models are plotted for F3 with $z_{\text{max}} = 0.2$, without peculiar velocity corrections and with a 250 km s^{-1} velocity dispersion for SNe.

Motivations
○○○○○

Relat. corr. with adapted coords.
○○○○○○○○○○○○○○○○○○○○○○○○○○○○○○○○

Local universe inhomogeneity
○○○○○○○○○○○○○○○○○○○○●○○○○○

Conclusions
○○

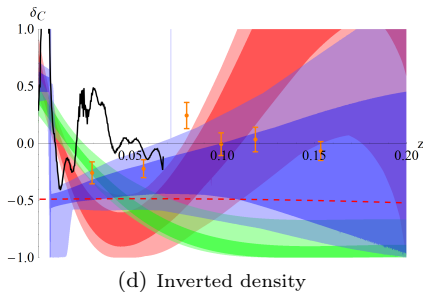
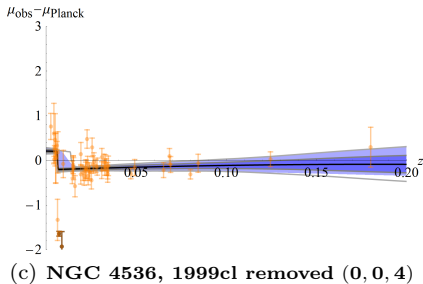
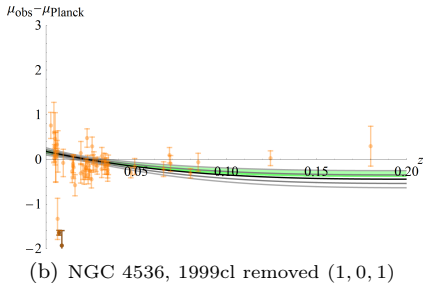
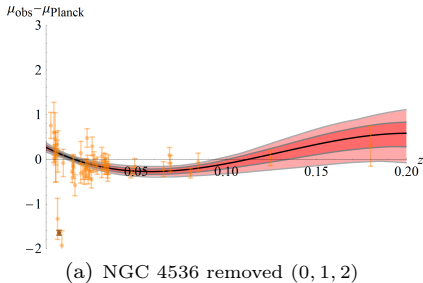
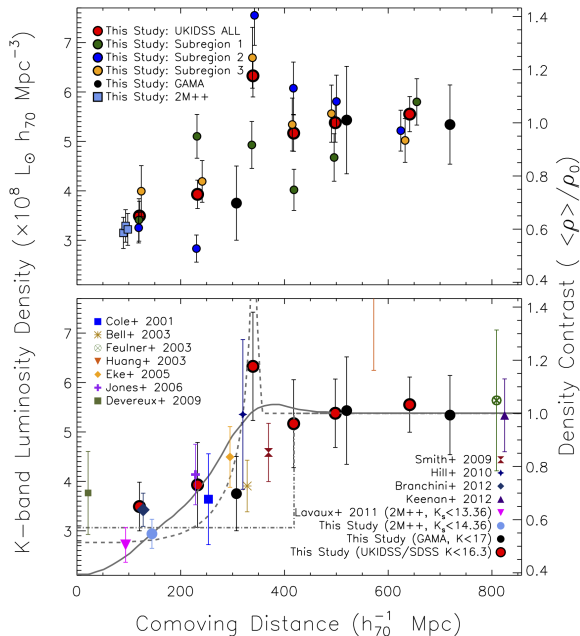


FIGURE: Distance modulus best fit models are plotted for F3 with $z_{\text{max}} = 0.4$, without peculiar velocity corrections and with a 250 km s^{-1} velocity dispersion for SNe.

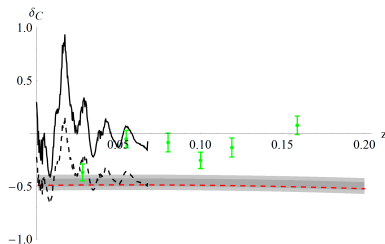
Comparison with
density maps obtained
from luminosity density of
Keenan et al. 2013.

- Green : Field 1
- Blue : Field 2
- Orange : Field 3

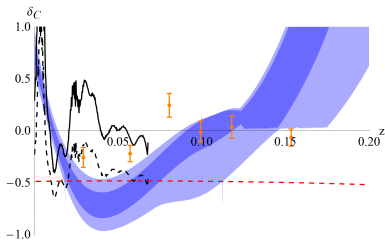
Keenan '13 suggests
2M++ **rescaling of**
 $\sim 0.6 \Rightarrow$ our density
matches quite well with
2M++ for such a
rescaling in F1, F3.



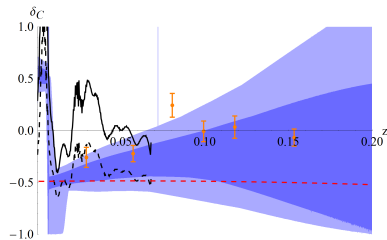
Main results



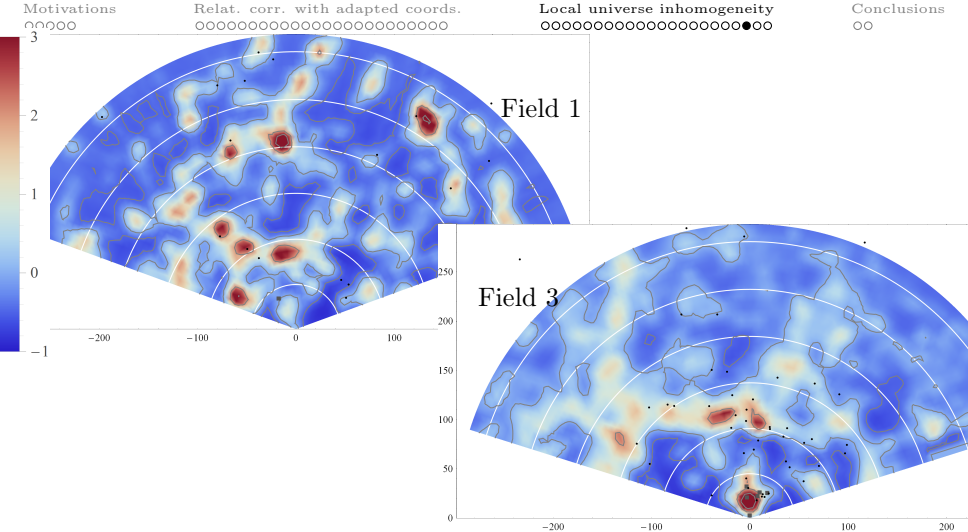
(a) Field 1, (1, 0, 0)



(b) Field 3, $z_{\max} = 0.2$ with NGC 4536 and 1999cl removed (0, 0, 2)



(c) Field 3, $z_{\max} = 0.4$ with NGC 4536 and 1999cl removed (0, 0, 4)



Comparison with 2M++ density map (averaged along declination direction in ICRS coordinates).

White arcs correspond to $z = 0.01, 0.02, \dots, 0.06$, gray contours indicate iso-density lines of $\delta_C = -0.5, 0, 2, 4$. Depth of the survey $R_{\text{max}} = 200 h^{-1} \text{Mpc}$, i.e. $z = 0.067$.

Rescaling 2M++

- 2M++ is normalized wrt the average within its depth \Rightarrow its normalization can be wrong if 2M++ is embedded in a larger structure.
- Same with Keenan 2013 with background equal to the averaged luminosity density over the data set.
- **Our reconstructed density profile is normalized wrt the background** since we are assuming cosmological background parameters obtained from large scale observations (Planck).

If we take $\mathcal{K}13$ background density we would have to rescale 2M++ as

$$\delta_C^{\text{cor}} = \frac{\tilde{\rho}_{2\text{M}++}}{\tilde{\rho}_{\mathcal{K}13}}(1 + \delta_C) - 1,$$

where δ_C^{cor} is the rescaled density contrast, while $\tilde{\rho}_{2\text{M}++}$ and $\tilde{\rho}_{\mathcal{K}13}$ are the assumed background density of 2M++ and $\mathcal{K}13 \Rightarrow$ **factor 0.6 rescaling**.

Our results :

- independently confirms the existence of inhomogeneities,
- to some extent in qualitative agreement with Keenan 2013 (claiming ~ 300 Mpc void), but normalization of background seems crucial,
- based on 1D fit in windows of the sky, LTB inversion model, with SNe Ia and Cepheids data \Rightarrow different sources of uncertainty,
- SNe Ia could be useful to correctly normalize density maps from galaxy surveys with respect to the average density of the Universe,
- could clarify the apparent discrepancy between local and large scale estimations of the H_0 (especially between Planck and Riess, which uses 2M++).

Conclusions

We have tools to work with **relativistic effects** in the large scale structure.
Adapted coordinates is one of them :

- GLC coordinates are convenient for many applications,
- they can be related to double-null coordinates (via DLC coordinates),
- there are still applications to explore,

in order to go below **percent accuracy** in cosmology.

But tools are not everything, we also have to **understand what we measure** :

- SNe are messy (and not classified!),
- H_0 tension is a big problem to solve! (before/with DE?),
- we need to better understand our local Universe,

as discoveries now hide **into the details**.

Motivations
○○○○○

Relat. corr. with adapted coords.
○○○○○○○○○○○○○○○○○○○○○○○○○○○○○○

Local universe inhomogeneity
○○○○○○○○○○○○○○○○○○○○○○○○○○○○○○

Conclusions
○●

Thank You!